PHOTONICS Research

Graphene-based saturable absorber and mode-locked laser behaviors under gamma-ray radiation

Dohyun Kim,[1,†] Nam Hun Park,[2,†] Hyunju Lee,[2] Jaegoan Lee,[1] Dong-Il Yeom,[2,3] and Jungwon Kim[1,*]

[1]School of Mechanical and Aerospace Engineering, Korea Advanced Institute of Science and Technology (KAIST), Daejeon 34141, South Korea
[2]Department of Energy Systems Research & Department of Physics, Ajou University, Suwon 16499, South Korea
[3]e-mail: diyeom@ajou.ac.kr
*Corresponding author: jungwon.kim@kaist.ac.kr

Received 22 February 2019; revised 19 April 2019; accepted 30 April 2019; posted 6 May 2019 (Doc. ID 360716); published 7 June 2019

We investigate optical and electrical behaviors of a graphene saturable absorber (SA) and mode-locking performance of a graphene-SA-based mode-locked Er fiber laser in gamma-ray radiation. When irradiated up to 4.8 kGy at ∼100 Gy/hr dose rate, the overall nonlinear transmittance in transverse electric mode was increased, while maintaining modulation depth to >10%. The corresponding polarization-dependent loss was reduced at a 1.2-dB/kGy rate. In the electrical properties, the charge carrier mobility was reduced, and the Dirac voltage shift was increased to positive under gamma-ray radiation. The radiation-induced optical and electrical changes turned out to be almost recovered after a few days. In addition, we confirmed that the graphene-SA-based laser showed stable CW mode-locking operation while the inserted graphene SA was irradiated for 2-kGy at a 45-Gy/hr dose rate, which corresponds to >40 years of operation in low Earth orbit satellites. To the best of our knowledge, this is the first evaluation of graphene SAs and graphene-SA-based mode-locked lasers in gamma-ray radiation, and the measured results confirm the high potential of graphene SAs and graphene-SA-based lasers in various outer-space environments as well as other radiation environments, including particle accelerators and radiation-based medical instruments.

https://doi.org/10.1364/PRJ.7.000742

1. INTRODUCTION

As femtosecond mode-locked lasers and optical frequency combs have advantages in precise time/frequency metrology due to their large spectral bandwidth and ultra-low noise, there have been emerging interests in space-borne applications of such laser sources, ranging from fundamental physics [1,2] through precision metrology [3,4] to navigation [5]. In particular, mode-locked fiber lasers, with their compactness, alignment-free operation, and light weight, are highly suitable for serving for space-borne applications. Recently, a mode-locked fiber laser oscillator and a fiber frequency comb have been successfully loaded on a low Earth orbit satellite [6] and a sounding rocket [7], respectively. These recent demonstrations show the potential of fiber-based mode-locked lasers and frequency combs as satellite payloads.

To maintain stable and ultrashort pulses from mode-locked lasers in space environments, a saturable absorber (SA) has to be robust against radiation. The SAs based on Kerr nonlinearity, such as a nonlinear amplifying loop mirror, could be easily affected by optical fiber attenuation due to their intensity-dependent performance. An optical fiber has radiation-induced attenuation (RIA), which depends on radiation energy, dose rate, exposure time, and temperature. In gamma-ray radiation, a standard single-mode fiber and an Er fiber show 7 dB/km [8] and ∼10 dB/m [9] attenuation at ∼25°C with 1 kGy radiation at 44.3 Gy/hr and 36 Gy/hr dose rates, respectively. Note that the gain fiber also includes a gain degradation (∼5 dB in an Er fiber for 1 kGy radiation at 32 Gy/hr dose rate [10]), which makes the Kerr-nonlinearity-based SAs more sensitive to radiation. On the other hand, real SA performances are determined by the properties of saturable absorption materials such as semiconductors, carbon-based materials (graphene, carbon nanotubes), and topological insulators. Thus, using real SA devices based on radiation-resistant materials could be more effective for mode-locked lasers in radiation.

So far, radiation tests of SAs and mode-locked lasers have been performed only for semiconductor saturable absorber mirrors (SESAMs). The SESAM showed a sudden degradation of its optical performance at 1.2 kGy in gamma-ray radiation because of defects developed in semiconductor layers during radiation [11]. The SESAM-based mode-locked lasers in radiation were examined as well [6,12].

Graphene, a single layer of carbon atoms formed in a hexagonal lattice, has attracted great interest from various

applications due to its unique optical and electrical properties [13–15]. In fiber laser systems, graphene has been one of the most promising materials for a mode locker and ultrashort pulse generation [16–19]. Considering its atomic structure, graphene has minimal interaction with high-energy ions owing to its very small thickness and low nominal cross section [20]. From this characteristic, graphene also can be an attractive material for applications in radiation environments including outer space [21]. There have been several research efforts for characterization of graphene and graphene-based devices under high-energy radiation (100 kGy–3 MGy) [22–26]. Graphene showed defects such as vacancies and interstitials when irradiating high-energy particles beyond the damage threshold [22]. However, fewer defects are expected at few kGy radiation, which is the typical condition with proper shielding for satellite payload applications [27]. In addition, no radiation test has been performed for graphene SAs or graphene-SA-based mode-locked lasers so far.

In this paper, we investigate the behavior of graphene SAs and evaluate the performance of graphene-SA-based mode-locked lasers in gamma-ray radiation. During radiation at ~100 Gy/hr average dose rate, the graphene SA at low fluence in transverse electric (TE) mode showed an increased nonlinear transmittance (NLT) from 3.8% (no irradiation) to 14% (4.8 kGy irradiation), while maintaining its modulation depth to 10%–11% in the measurement range. The corresponding polarization-dependent loss (PDL) was reduced at 1.2 dB/kGy rate. In electrical properties, electron (hole) mobility was reduced to 16% (93%), and a Dirac voltage was shifted to +15 V after irradiation of 2.3 kGy. Such changes were almost recovered a few days after radiation. In addition, we confirmed that the mode-locked laser showed stable operation when the inserted graphene SA was irradiated for 2 kGy at 45 Gy/hr dose rate. This corresponds to the irradiation dose for ~40 years operation in low Earth orbit, which is much longer than the typical lifespan of satellites. Thus, the graphene SAs would be suitable for mode-locked lasers for satellite payloads and have potential for various applications in radiation environments.

2. PREPARATION OF THE DEVICE AND GAMMA-RAY IRRADIATION

For the SA under test, we used an evanescent-field interacting-type side-polished fiber as an SA platform [see Fig. 1(a)]. A monolayer graphene was grown on a copper foil by the chemical vapor deposition method [28] and coated with polymethylmethacrylate (PMMA) film, which was used as a supporting layer. The copper foil was etched by using an ammonium persulfate solution and the graphene/PMMA layer then transferred onto the side-polished fiber embedded in a grooved quartz block. The PMMA supporting layer was then removed by acetone. Since a monolayer graphene-based SA has a low modulation depth (<1%) and little polarization dependence, an over-cladding layer was introduced on the graphene layer to enhance interaction between graphene and light [18]. Here, we used an index-matched ultra-violet (UV) cured polymer as the over-cladding layer.

A standard back-gated graphene field effect transistor (FET) was fabricated as schematically shown in Fig. 1(b) to investigate

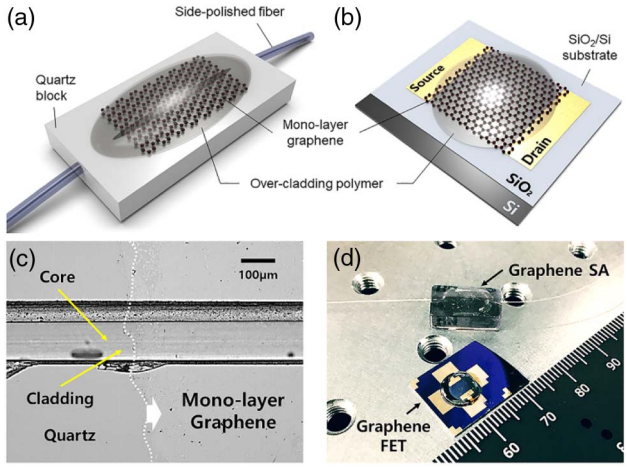

Fig. 1. (a) Schematic of the graphene SA with a UV-cured polymer over-cladding on the monolayer graphene sheet and (b) back-gated graphene FET including the over-cladding. (c) Optical microscope image of the graphene SA at the edge of interaction region. (d) Photo of the devices.

electrical behavior under radiation. A graphene sheet, fabricated in the same manner as the graphene SA, was transferred onto the silica/silicon substrate. The graphene layer, which acts as a channel, was then connected to source and drain electrodes to characterize the electrical response at applied back-gated voltage. The fabricated graphene FET was also covered with UV-cured polymer, the same as used in the graphene SA for parallel comparison.

To investigate how the graphene SA behaves in radiation environments, the radiation test was conducted at the $_{60}$Co facility at KAERI-ARTI (Jeongeup, South Korea). The temperature in the radiation room was 28–29°C during the test. The graphene SA was irradiated up to 6.7 kGy at a 98 Gy/hr dose rate, referring to Refs. [6,11].

3. OPTICAL PROPERTIES OF GRAPHENE SA IN GAMMA-RAY RADIATION

We first examined the optical properties of the graphene SA in radiation of gamma rays. The optical properties were measured when irradiated to 0 kGy, 2.5 kGy, 4.8 kGy, and 6.7 kGy, using a femtosecond pulse and a continuous-wave (CW) light. By adjusting an input polarization state, we measured the optical properties in TE and transverse magnetic (TM) modes. Note that the NLT of 6.7 kGy-irradiated graphene SA was measured three days after radiation without any special treatment.

As a pulse source, we used a lab-built polarization-maintaining Er fiber laser with 34 MHz repetition rate and ~300 fs pulse duration. The incident fluence was modulated in the range of 1–1000 μJ/cm^2 by an optical attenuator. To observe the radiation-induced changes of optical properties, we evaluated the modulation depth and the saturation fluence from the NLT curve, which are important to determine the SA performance.

The fabricated graphene SA under test had 3.8% NLT at low fluence (~5 μJ/cm^2) and 10% modulation depth in TE mode, whose polarization of the light is parallel to the graphene

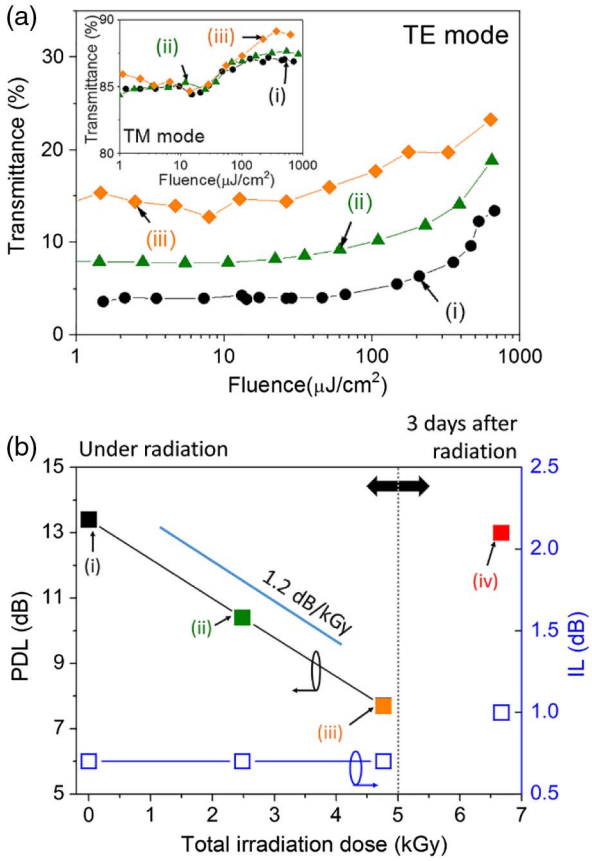

Fig. 2. (a) NLT of the graphene SA measured by the femtosecond pulses in TE mode (inset: NLT in TM mode). (b) PDL and IL of the graphene SA as a function of irradiation dose measured by the CW light. (i) 0 kGy, (ii) 2.5 kGy, (iii) 4.8 kGy, and (iv) 6.7 kGy at 98 Gy/hr average dose rate. Note that the 6.7 kGy-irradiated sample (iv) was measured three days after radiation (without any special treatment), showing the recovery property in PDL.

layer [curve (i) in Fig. 2(a)]. On the other hand, in TM mode where the light hardly interacts with the graphene, the NLT was 85% at low fluence, and the modulation depth was 2%.

As shown in Fig. 2(a), the overall NLT curve in TE mode was increased by radiation, showing an increase of NLT at low fluence (~5 μJ/cm^2): 3.8%, 7.8%, and 14% at 0 kGy, 2.5 kGy, and 4.8 kGy irradiation dose, respectively. The modulation depths in TE mode, in the measurement range, were maintained at 10%–11%. There were no noticeable changes in the NLT curves in TM mode. They showed constant modulation depths in 2%–3%. Since the saturation was not observed in the measurement range, we fitted the curves to the equation in Ref. [29] for the estimation of the saturation fluence:

$$q(S) = \frac{q_s}{\sqrt{S(1+S)}} \operatorname{arctanh}\left(\sqrt{\frac{S}{1+S}}\right) + q_{ns}, \quad (1)$$

where q_s is the saturated loss, q_{ns} is the nonsaturable loss, and S is the ratio of the peak intensity to the saturation intensity.

From this calculation, the saturation fluence was 8298 μJ/cm^2, 6522 μJ/cm^2, and 391.3 μJ/cm^2 at 0 kGy, 2.5 kGy, and 4.8 kGy irradiation, respectively. Although the saturation fluence was reduced, the modulation depth was still larger than 10%. As a result, the graphene SA showed >10% modulation depth even at 4.8 kGy irradiation, whereas the SESAM showed sudden changes in its modulation depth and saturation fluence at 1.2 kGy [11]. In addition, in contrast to the SESAM, the NLT curve was increased in TE mode under radiation. This graphene SA behavior enables robust operation of mode-locked lasers in spite of the RIA of fiber.

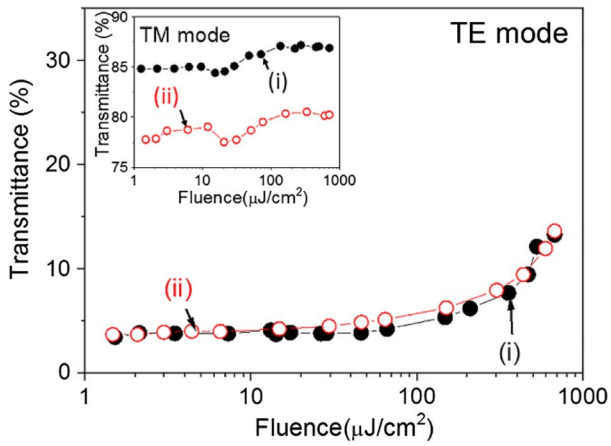

Fig. 3. Measured NLT curve of the graphene SA in TE mode (i) before radiation and (ii) three days after radiation of 6.7 kGy (inset: NLT curve in TM mode). Note that there was no special treatment for three days.

The PDL and the insertion loss (IL) of the graphene SA shown in Fig. 2(b) were measured by the CW light as well. The incident power was −2 dBm. Before radiation, the PDL and IL were 13.4 dB and 0.7 dB, respectively. The PDL was reduced by a 1.2 dB/kGy rate from 13.4 dB (no irradiation) to 7.7 dB (4.8 kGy irradiation), while the IL was kept almost uniform.

Interestingly, the NLT curve showed recovery behavior, after the irradiated SA was placed in a laboratory environment for three days without any special treatment. The NLT curve was almost recovered to un-radiated condition—even irradiated up to 6.7 kGy (4.0% at ~5 μJ/cm^2, see curve (ii) in Fig. 3). This indicates that the increase of NLT curve by radiation is not a permanent change. In Fig. 2(b), there is a slightly increased IL from 0.7 dB to 1.0 dB after radiation, while the PDL is almost recovered to 13 dB. It seems that the radiation-induced PDL reduction affects an IL increase in the process of self-healing after radiation.

4. ELECTRICAL PROPERTIES OF GRAPHENE SA IN GAMMA-RAY RADIATION

The graphene SAs integrated with FETs can manipulate their NLT characteristics electrically by active control of gating, as recently reported in Ref. [19]. Thus, we also investigated the electrical behavior of graphene FETs [Fig. 1(b)] under radiation. The transfer characteristics of the back-gated graphene FET were measured after 0 kGy, 2.3 kGy, and 4.2 kGy irradiation [curves (i)–(iii) in Fig. 4] at a 95 Gy/hr

dose rate. Note that the data irradiated to 4.2 kGy [curve (iii) in Fig. 4] were measured four days after radiation without any treatment.

After 2.3 kGy irradiation, we observed that the average electron (hole) mobility of the graphene FET was changed to 16% (93%) with the Dirac voltage shift of +15 V as shown in curve (ii) in Fig. 4. This tendency of shifted Dirac voltage to the positive direction with reduced mobility reasonably agrees with that of a previous observation of gamma-ray-radiated graphene FET [25]. Moreover, the change of electrical properties at 4.2 kGy irradiation was observed to be almost recovered, when measured after a few days. The average electron (hole) mobility and the Dirac voltage were recovered back to 45% (108%) and +1.5 V of the non-radiated results, respectively, as shown in curve (iii) in Fig. 4. Note that this recovered behavior was not observed in the previous study [25] where the device was exposed under much stronger gamma-ray radiation of 200 kGy than ours (4.2 kGy). Thus, we expect that a permanent damage or defect is rarely built up at the graphene layer in our gamma-ray radiation condition. Such recovery can make the graphene SAs robust at sudden strong radiation impacts such as solar activity [30]. Moreover, with further research of NLT behaviors in gating control under radiation, the NLT characteristics of graphene SAs can be controlled to slow down their radiation-induced changes.

To identify graphene layer damages under radiation, the Raman spectra of our sample were measured for different radiation conditions. As shown in Fig. 5, we observed that there was no significant change in Raman spectra under irradiations except for a slight increase in defect peak at 1344.4 cm^{-1}. This tendency reasonably agrees with the result previously reported [25], and we expect that such small variation in defect signal does not seriously affect the property of the SA.

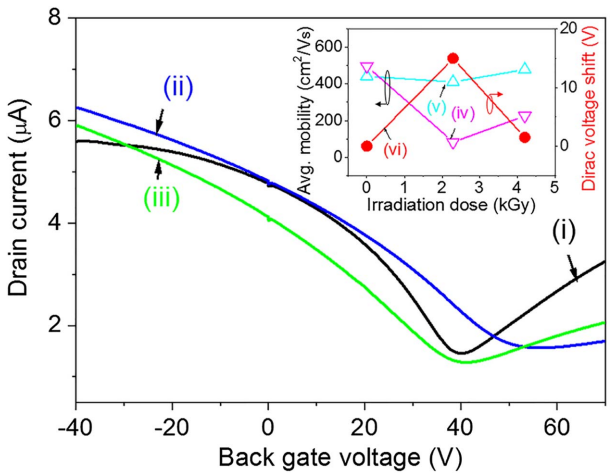

Fig. 4. Measured transfer characteristics of the back-gated graphene FET including the over-cladding layer. The results are for (i) 0 kGy, (ii) 2.3 kGy, and (iii) 4.2 kGy at a 95 Gy/hr dose rate [inset: changes of the average charge carriers mobility [(iv) electron and (v) hole] and (vi) the Dirac voltage of the graphene FET as a function of irradiation dose]. Note that the result of 4.2 kGy irradiation (iii) was measured four days after radiation without any special treatment.

5. GRAPHENE SA MODE-LOCKED LASER OPERATION IN GAMMA-RAY RADIATION

In addition, the mode-locked laser performance was measured during irradiation to see how the irradiated graphene SA affects the laser. The laser under test was a 37-MHz-repetition-rate Er fiber laser mode locked by the graphene SA. In order to realize a stable mode-locked fiber laser, a ring laser cavity using a hybrid component consisting of an output coupler, a wavelength division multiplexer (WDM), and an isolator was built as schematically described in Fig. 6(b). An Er fiber of 1 m was pumped by a 976 nm laser diode, and a polarization controller was used to control the polarization state of the light in the fiber laser. The total cavity length was measured to be 5.6 m, where the estimated total cavity dispersion was −0.11 ps^2. The output power was 2.35 at 150 mW pump power. We confirmed that the laser maintained stable mode-locking condition for more than several days.

The inserted graphene SA had 9% NLT at low fluence in TE mode and 8% modulation depth before radiation. The PDL and IL were measured to be 10 dB and 0.7 dB, respectively. In order to see the radiation-induced effects of only the graphene SA in the laser, radiation to the other laser components (in particular, the gain fiber) was minimized. The inserted graphene SA was irradiated at 45 Gy/hr dose rate, while the remaining parts of the laser were irradiated with 3.4% of the irradiation dose to the graphene SA by using lead blocks [shown in Fig. 6(a)]. The corresponding total irradiation dose of the graphene SA and the rest of the laser was 1.98 kGy and 67 Gy, respectively. By ∼2 kGy radiation, the graphene SA was estimated to show an increased NLT curve (from 9% to ∼15% at low fluence) in TE mode and ∼2.5 dB reduction in PDL (when referring to the results shown in Fig. 2).

Figures 7(a) and 7(b) show the optical spectra and photodetected pulse trains, respectively, when measured at 0 kGy, 0.5 kGy, 1.0 kGy, 1.5 kGy, and 1.98 kGy irradiation doses. In the optical spectra, the center wavelength is shifted to shorter wavelength as radiation dose increases [see Fig. 7(a)]. Up to 1.98 kGy irradiation, the center wavelength shifted by ∼2 nm, while the full width at half-maximum (FWHM)

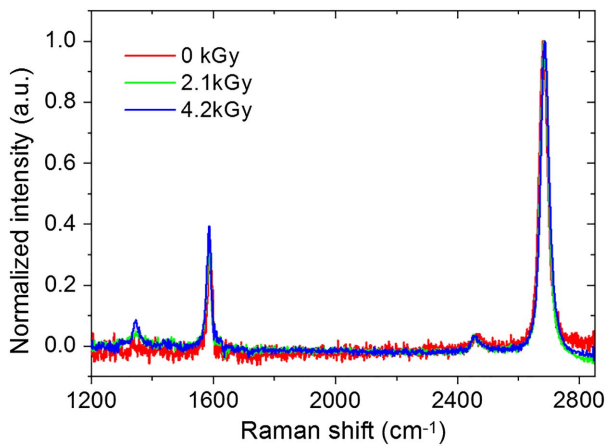

Fig. 5. Measured Raman spectra of our sample under different radiation conditions (0 kGy, 2.1 kGy, and 4.2 kGy).

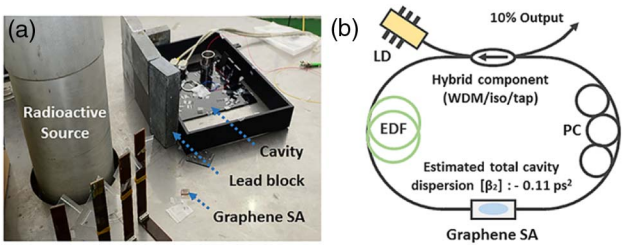

Fig. 6. (a) Photo of the radiation test setup of the mode-locked laser. Note that the rest of the parts in the laser except the graphene SA were irradiated with a lower dose (3.4% of the irradiation dose to the graphene SA). (b) Schematic of the laser under test. EDF, Er-doped fiber; LD, pump laser diode; PC, polarization controller.

bandwidth was maintained at ~3 nm. In addition, the time-domain pulse trains were measured by a 2 GHz InGaAs photodetector (EOT, ET-3010) followed by a 1 GHz oscilloscope (Agilent, DSO6104A). For all radiation conditions, the time-domain pulse trains were measured to be almost identical, as shown in Fig. 7(b). Thus, the laser under test maintained stable CW mode-locking performance up to ~2 kGy irradiation to the graphene SA, which is sufficient to operate in low Earth orbit satellites (typ. ~250 Gy radiation during their life span) [31]. Note that the radiation was not proceeded more than 2 kGy due to the limited time of use of the facility.

The average optical power (after 3 dB coupler from the output) was simultaneously measured during radiation as shown in Fig. 7(c). There was 2.4 dB output power reduction during radiation due to RIA of the optical fiber (especially, Er fiber) and SA degradation. The estimated RIA of a standard single-mode fiber and an Er fiber at corresponding irradiation is ~0.002 dB [8] and ~1 dB [9], respectively. After the radiation-induced change in the NLT was fully recovered, the output power was still 1.6 dB lower than the measured power before radiation. Note that, after radiation, the laser required higher pump power (170 mW) to mode-lock due to gain degradation of the Er fiber [10,27]. As a result, 1.5 dB of loss was caused by the fiber RIA, since the IL of the graphene SA was increased from 0.7 dB to 0.8 dB, when the PDL was recovered after radiation, as shown in Fig. 3. This is similar to the RIA observed in the previous study of a SESAM-based mode-locked fiber laser (at the corresponding irradiation dose) [6]. Therefore, 0.9 dB power loss was due to graphene SA degradation by ~2 kGy irradiation, which is not permanent damage. The irradiation dose to the SA, when stable mode-locking was maintained, corresponded to the exposure of radiation for 41.3 years in low Earth orbit [6] and 28.3 years in geostationary orbit (in a 3 mm aluminum shield) [32]. Thus, the graphene-SA-based lasers would be feasible in both low Earth and geostationary orbits, as they can sustain more than the life span of satellites [27,33]. In addition, graphene-SA-based lasers and devices will be promising in other radiation environments such as particle accelerators and radiation-based medical instruments [34].

6. CONCLUSION

In summary, we have investigated radiation-induced changes in optical and electrical properties of the graphene SA in gamma-ray radiation. We also monitored the mode-locked laser performance while the graphene SA in the laser was irradiated up to 2 kGy irradiation dose. When irradiated at ~100 Gy/hr average dose rate, the NLT of the graphene SA in TE mode was increased as the NLT at low fluence was changed from 3.8% (no irradiation) to 14% (4.8 kGy irradiation). During radiation, the PDL of the graphene SA was reduced by a 1.2 dB/kGy rate. However, the modulation depth in the measurement range (1–1000 $\mu J/cm^2$) was maintained at ~10% even irradiated up to 4.8 kGy, while the SESAM showed sudden changes at 1.2 kGy. The average electron (hole) mobility and the Dirac voltage of the graphene FET showed an 84% (7%) reduction and +15 V shift, respectively, at 2.3 kGy irradiation. Interestingly, the optical and electrical changes induced by radiation up to several kGy were not permanent and mostly recovered after a few days. In addition, we confirmed that the graphene-SA-based mode-locked laser maintained stable CW mode-locking condition when the graphene SA was irradiated up to 2 kGy, which is the irradiation dose of ~40 years' operation in low Earth-orbit satellites. From our investigation results, we believe that graphene-SA-based optical/electronic devices and mode-locked lasers are highly suitable for space-borne applications as well as various radiation environments, e.g., in particle accelerators and accelerator-based medical instruments.

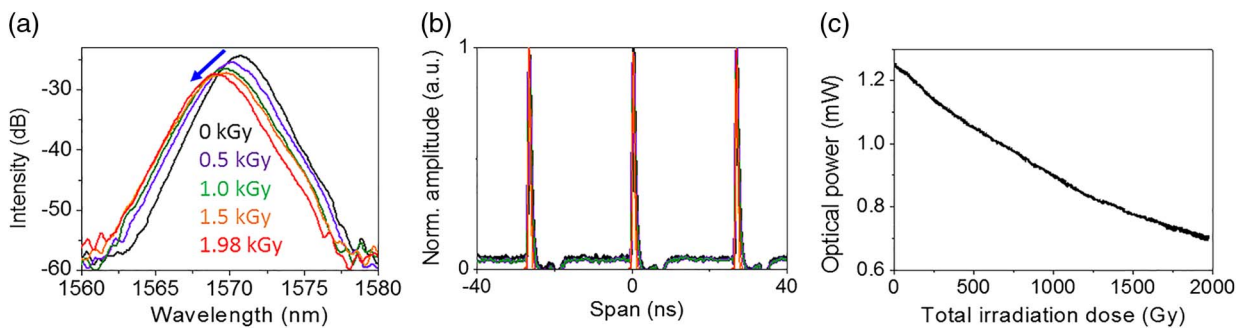

Fig. 7. (a) Optical spectra and (b) time-domain photodetected pulse trains of the mode-locked laser for different radiation conditions (0 kGy, 0.5 kGy, 1.0 kGy, 1.5 kGy, and 1.98 kGy). (c) Average optical power change of the mode-locked laser while the graphene SA was irradiated at a 45 Gy/hr dose rate.

Funding. National Research Foundation of Korea (NRF) (2016R1A2B2012281, 2018R1A2B3001793).

[†]These authors contributed equally to this work.

REFERENCES

1. A. Derevianko and M. Pospelov, "Hunting for topological dark matter with atomic clocks," Nat. Phys. **10**, 933–936 (2014).
2. S. Kolkowitz, I. Pikovski, N. Langellier, M. D. Lukin, R. L. Walsworth, and J. Ye, "Gravitational wave detection with optical lattice atomic clocks," Phys. Rev. D **94**, 124043 (2016).
3. T. Udem, R. Holzwarth, and T. W. Hänsch, "Optical frequency metrology," Nature **416**, 233–237 (2002).
4. T. Steinmetz, T. Wilken, C. Araujo-Hauck, R. Holzwarth, T. W. Hänsch, L. Pasquini, A. Manescau, S. D'Odorico, M. T. Murphy, T. Kentischer, W. Schmidt, and T. Udem, "Laser frequency combs for astronomical observations," Science **321**, 1335–1337 (2008).
5. J. A. Stone and P. Egan, "An optical frequency comb tied to GPS for laser frequency/wavelength calibration," J. Res. Natl. Inst. Stand. Technol. **115**, 413–431 (2010).
6. J. Lee, K. Lee, Y.-S. Jang, H. Jang, S. Han, S.-H. Lee, K.-I. Kang, C.-W. Lim, Y.-J. Kim, and S.-W. Kim, "Testing of a femtosecond pulse laser in outer space," Sci. Rep. **4**, 5134 (2014).
7. M. Lezius, T. Wilken, C. Deutsch, M. Giunta, O. Mandel, A. Thaller, V. Schkolnik, M. Schiemangk, A. Dinkelaker, A. Kohfeldt, A. Wicht, M. Krutzik, A. Peters, O. Hellmig, H. Duncker, K. Sengstock, P. Windpassinger, K. Lampmann, T. Hülsing, T. W. Hänsch, and R. Holzwarth, "Space-borne frequency comb metrology," Optica **3**, 1381–1387 (2016).
8. M. N. Ott, "Radiation effects data on commercially available optical fiber: database summary," in *Proceedings of IEEE Radiation Effects Data Workshop* (IEEE, 2002), pp. 24–31.
9. M. Lezius, K. Predehl, W. Stöwer, A. Türler, M. Greiter, C. Hoeschen, P. Thirolf, W. Assmann, D. Habs, A. Prokofiev, C. Ekström, T. W. Hänsch, and R. Holzwarth, "Radiation induced absorption in rare earth doped optical fibers," IEEE Trans. Nucl. Sci. **59**, 425–433 (2012).
10. O. Berné, M. Caussanel, and O. Gilard, "A model for the prediction of EDFA gain in a space radiation environment," IEEE Photon. Technol. Lett. **16**, 2227–2229 (2004).
11. Y.-S. Jang, J. Lee, S. Kim, K. Lee, S. Han, Y.-J. Kim, and S.-W. Kim, "Space radiation test of saturable absorber for femtosecond laser," Opt. Lett. **39**, 2831–2834 (2014).
12. G. Buchs, S. Kundermann, E. Portuondo-Campa, and S. Lecomte, "Radiation hard mode-locked laser suitable as a spaceborne frequency comb," Opt. Express **23**, 9890–9900 (2015).
13. F. Bonaccorso, Z. Sun, T. Hasan, and A. C. Ferrari, "Graphene photonics and optoelectronics," Nat. Photonics **4**, 611–622 (2010).
14. A. K. Geim and K. S. Novoselov, "The rise of graphene," Nat. Mater. **6**, 183–191 (2007).
15. A. N. Grigorenko, M. Polini, and K. S. Novoselov, "Graphene plasmonics," Nat. Photonics **6**, 749–758 (2012).
16. Z. Sun, T. Hasan, F. Torrisi, D. Popa, G. Privitera, F. Wang, F. Bonaccorso, D. M. Basko, and A. C. Ferrari, "Graphene mode-locked ultrafast laser," ACS Nano **4**, 803–810 (2010).
17. G. Sobon, J. Sotor, and K. M. Abramski, "All-polarization maintaining femtosecond Er-doped fiber laser mode-locked by graphene saturable absorber," Laser Phys. Lett. **9**, 581–586 (2012).
18. N. H. Park, H. Jeong, S. Y. Choi, M. H. Kim, F. Rotermund, and D.-I. Yeom, "Monolayer graphene saturable absorbers with strongly enhanced evanescent-field interaction for ultrafast fiber laser mode-locking," Opt. Express **23**, 19806–19812 (2015).
19. E. J. Lee, S. Y. Choi, H. Jeong, N. H. Park, W. Yim, M. H. Kim, J.-K. Park, S. Son, S. Bae, S. J. Kim, K. Lee, Y. H. Ahn, K. J. Ahn, B. H. Hong, J.-Y. Park, F. Rotermund, and D.-I. Yeom, "Active control of all-fibre graphene devices with electrical gating," Nat. Commun. **6**, 6851 (2015).
20. E. H. Åhlgren, J. Kotakoski, O. Lehtinen, and A. V. Krasheninnikov, "Ion irradiation tolerance of graphene as studied by atomistic simulations," Appl. Phys. Lett. **100**, 233108 (2012).
21. E. J. Siochi, "Graphene in the sky and beyond," Nat. Nanotechnol. **9**, 745–747 (2014).
22. Y. Wang, Y. Feng, F. Mo, G. Qian, Y. Chen, D. Yu, Y. Wang, and X. Zhang, "Influence of irradiation upon few-layered graphene using electron-beams and gamma-rays," Appl. Phys. Lett. **105**, 023102 (2014).
23. A. Ansón-Casaos, J. A. Puértolas, F. J. Pascual, J. Hernández-Ferrer, P. Castell, A. M. Benito, W. K. Maser, and M. T. Martínez, "The effect of gamma-irradiation on few-layered graphene materials," Appl. Surf. Sci. **301**, 264–272 (2014).
24. D. N. Kleut, Z. M. Marković, I. D. H. Antunović, M. D. Dramićanin, D. P. Kepić, and B. M. T. Marković, "Gamma ray-assisted irradiation of few-layer graphene films: a Raman spectroscopy study," Phys. Scr. **T162**, 014025 (2014).
25. K. Alexandrou, A. Masurkar, H. Edrees, J. F. Wishart, Y. Hao, N. Petrone, J. Hone, and I. Kymissis, "Improving the radiation hardness of graphene field effect transistors," Appl. Phys. Lett. **109**, 153108 (2016).
26. A. Patil, O. Koybasi, G. Lopez, M. Foxe, I. Childres, C. Roecker, J. Boguski, J. Gu, M. L. Bolen, M. A. Capano, P. Ye, I. Jovanovic, and Y. P. Chen, "Graphene field effect transistor as radiation sensor," in *IEEE Nuclear Science Symposium Conference Record* (2011), pp. 455–459.
27. S. Girard, A. Morana, A. Ladaci, T. Robin, L. Mescia, J.-J. Bonnefois, M. Boutillier, J. Mekki, A. Paveau, B. Cadier, E. Marin, Y. Ouerdane, and A. Boukenter, "Recent advances in radiation-hardened fiber-based technologies for space applications," J. Opt. **20**, 093001 (2018).
28. K. S. Kim, Y. Zhao, H. Jang, S. Y. Lee, J. M. Kim, K. S. Kim, J.-H. Ahn, P. Kim, J.-Y. Choi, and B. H. Hong, "Large-scale pattern growth of graphene films for stretchable transparent electrodes," Nature **457**, 706–710 (2009).
29. C.-C. Lee, J. M. Miller, and T. R. Schibli, "Doping-induced changes in the saturable absorption of monolayer graphene," Appl. Phys. B **108**, 129–135 (2012).
30. M. H. MacAlester and W. Murtagh, "Extreme space weather impact: an emergency management perspective," Space Weather **12**, 530–537 (2014).
31. E. G. Stassinopoulos and J. P. Raymond, "The space radiation environment for electronics," Proc. IEEE **76**, 1423–1442 (1988).
32. B. R. Bhat, N. Upadhyaya, and R. Kulkarni, "Total radiation dose at geostationary orbit," IEEE Trans. Nucl. Sci. **52**, 530–534 (2005).
33. P. Fortescue, G. Swinerd, and J. Stark, *Spacecraft Systems Engineering*, 4th ed. (Wiley, 2011), p. 399.
34. F. A. Mettler, W. Huda, T. T. Yoshizumi, and M. Mahesh, "Effective doses in radiology and diagnostic nuclear medicine: a catalog," Radiology **248**, 254–263 (2008).